



# Impedance and Ferroelectric Characterization of Silver Sodium Niobate Ceramic

Meenu Rani<sup>1</sup>, Y.P. Singh<sup>2</sup>, \*Shilpi Jindal<sup>3</sup>

<sup>1</sup>Department of Physics, Hindu College Sonipat

<sup>2</sup> Institute of Applied Sciences, Mangalayatan University, Beswan, Aligarh

<sup>3</sup> Department of Physics, Chandigarh University, Gharuan, Mohali\*

**ABSTRACT-** Silver Sodium Niobate  $\text{Ag}_{0.2}\text{Na}_{0.8}\text{NbO}_3$  (ANN) ceramic pellets had been synthesized by using solid state reaction approach to examine the impedance and ferroelectric properties. X-ray diffraction (XRD) established the structure of specimen to be perovskite orthorhombic. Scanning Electron Microscope (SEM) confirmed presence of grains with different size. Impedance analysis indicated a decrease in both real ( $Z'$ ) & imaginary ( $Z''$ ) part of impedance with rise in frequency as well as rise in temperature. Nyquist plot depicted that grain boundaries contribute dominantly over grains to conduction process. Moderate polarization & high coercive field observed in ferroelectric measurement revealed use of sample in making non-volatile memory devices.

**Keywords-** perovskite, impedance, ferroelectric, polarization

**1 INTRODUCTION-** Perovskites denoted in general by the formula  $\text{ABO}_3$  form a significant class of materials having important physical and chemical properties making them suitable choice for great practical applications. Sodium niobate ( $\text{NaNbO}_3$ ) is an important member of this group. Ceramics based on sodium niobate have been found to possess good electrical properties and they have been studied extensively. Dielectric property and polarization mechanism of rare earth doped sodium niobate based ceramics had been reported.[1] Structural & magnetic properties of Fe and Cu co-doped  $\text{NaNbO}_3$  ceramics had been investigated. [2] Study of Impedance and electrical properties of modified potassium sodium niobate had been done.[3] Sodium niobate had been studied for energy storage applications. [4] Tantalum doped  $\text{NaNbO}_3$  based ceramics had been investigated.[5] Investigation of structural, optical and magnetic properties of silver modified sodium niobate ceramics had been done. [6] In present work, silver sodium niobate ceramic had been synthesized to explore its impedance & ferroelectric properties.

**2 EXPERIMENTAL DETAILS-** Highly pure silver oxide ( $\text{Ag}_2\text{O}$ ), sodium carbonate ( $\text{Na}_2\text{CO}_3$ ) and niobium pentaoxide ( $\text{Nb}_2\text{O}_5$ ) were the raw materials used for preparation of silver sodium niobate with composition  $\text{Ag}_{0.2}\text{Na}_{0.8}\text{NbO}_3$  by solid-state reaction method. Raw materials were mixed, grounded and then calcined at  $1050^\circ$  for 2 hours. To this calcined mixture after grounding again, few drops of polyvinyl alcohol (PVA) had been added to convert it into disc shaped pellets with 10 mm diameter and 1 mm thickness applying 1 ton pressure using hydraulic press. After this step, sintering of pellets had been done at  $1150^\circ\text{C}$  for 1 hour. Phillips X-ray diffractometer with  $\text{Cu K}_\alpha$  radiations had been used to record XRD pattern of specimen. Surface morphology had been observed using Scanning Electron Microscope (SEM) (TESCAN VEGA III LM) along with EDX. For impedance and ferroelectric measurement, sintered pellets had been changed into capacitor form by application of thin silver paste on its both sides. Keysight Impedance analyzer E 4990 20 Hz- 20 MHz had been used for impedance analysis. Marine India instrument (Model: 20 PE 1 KHz 1 N) had been used to record Polarization-Electric field (P-E) loop corresponding to room temperature for ferroelectric measurement.

### 3 RESULTS AND DISCUSSION-

**3.1 Structural Analysis-** Figure 1 displays recorded XRD pattern of ANN specimen. Diffraction peaks has been indexed using Joint Committee on Powder Diffraction Standards data card n. 01-082-0606 ( $\text{NaNbO}_3$ ).[7] XRD data analysis reveals that sample possessed stable perovskite orthorhombic structure.

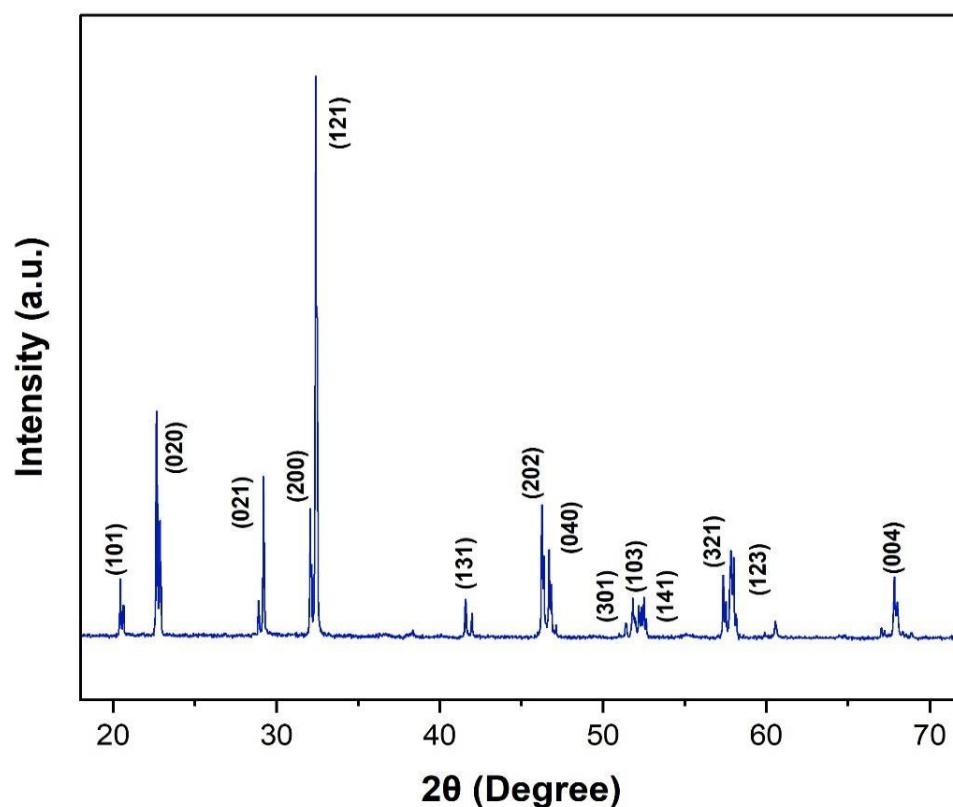


Figure 1: XRD pattern of  $\text{Ag}_{0.2}\text{Na}_{0.8}\text{NbO}_3$

**3.2 Microstructural Analysis-** Obtained SEM image of specimen as shown in figure 2(a) shows presence of grains having varying size with average grain size of  $1.69\ \mu\text{m}$  as calculated using ImageJ software. Recorded EDX spectrum as shown in figure 2(b) depicts that all required elements are present in sample.

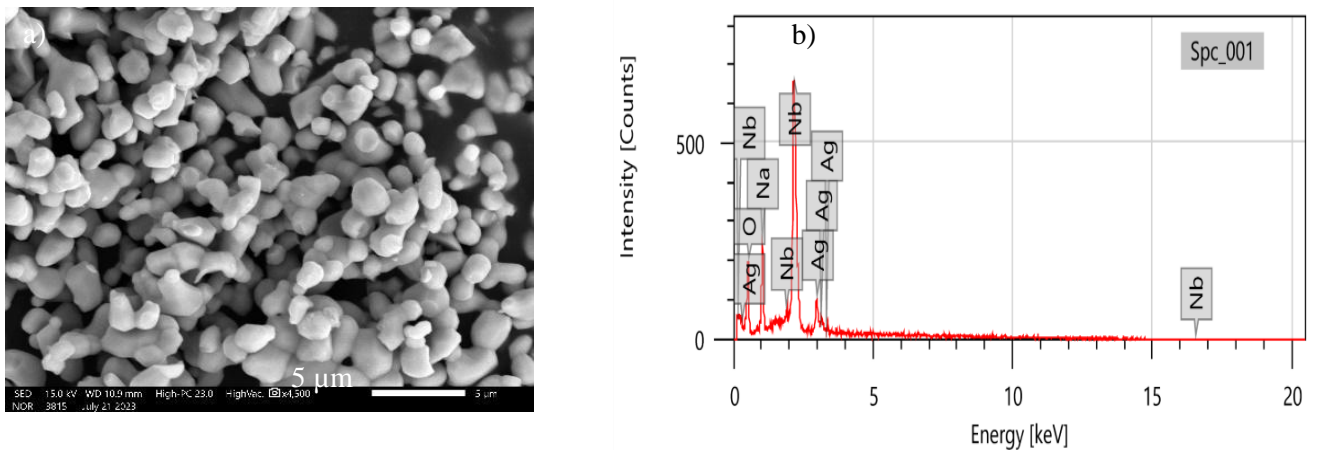


Figure 2: (a) SEM image, (b) EDX spectrum of  $\text{Ag}_{0.2}\text{Na}_{0.8}\text{NbO}_3$

**3.3 Impedance Analysis-** Impedance study is used to get information about role of grains and grain boundaries in conduction process. Figure 3 and figure 4 show dependence of real part ( $Z'$ ) and imaginary part ( $Z''$ ) of complex impedance on frequency at room temperature for prepared sample.

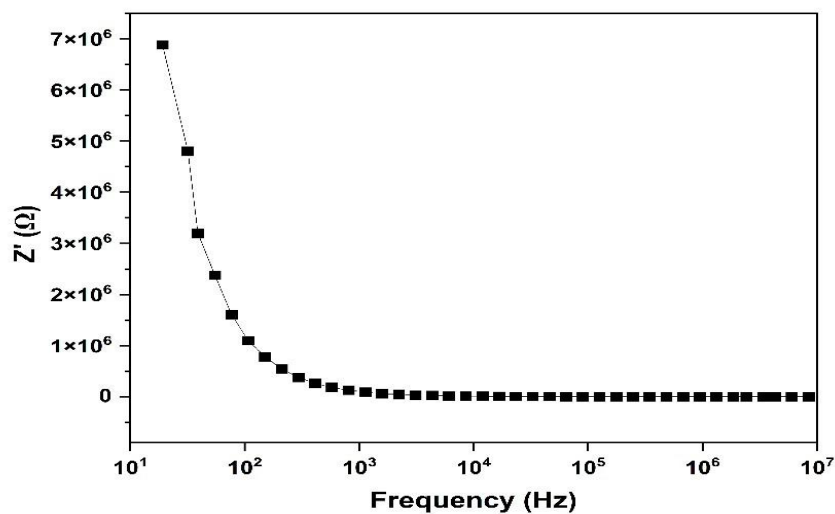


Figure 3: Variation of Real part ( $Z'$ ) of impedance with frequency for  $\text{Ag}_{0.2}\text{Na}_{0.8}\text{NbO}_3$  at room temperature

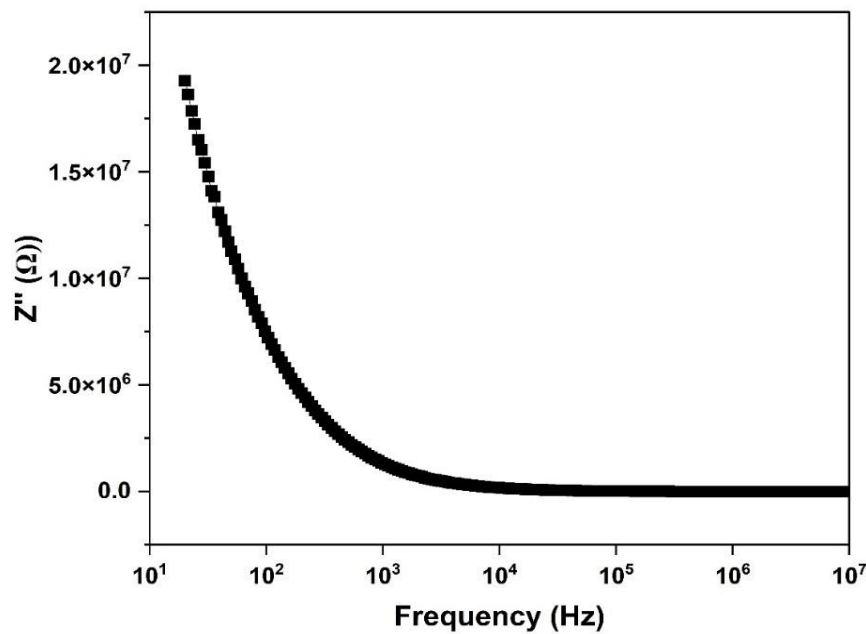


Figure 4: Variation of imaginary part ( $Z''$ ) of impedance with frequency for  $\text{Ag}_{0.2}\text{Na}_{0.8}\text{NbO}_3$  at room temperature.

As frequency increases,  $Z'$  is found to be decreasing and it becomes constant and almost zero at high frequencies. High  $Z'$  in low frequency region is due to presence of all types of polarizations namely electronic, ionic, orientational & space charge polarization and constant  $Z'$  at high frequencies is related to weakened space charge polarization at these frequencies. A rise in a.c. conductivity is revealed by declining trend of the  $Z'$  with frequency. The nature of variation of  $Z''$  with frequency as displayed in figure 4 is same as that of  $Z'$ . Evolution of  $Z'$  and  $Z''$  against frequency at different temperatures have been shown in respectively figure 5 & figure 6 .

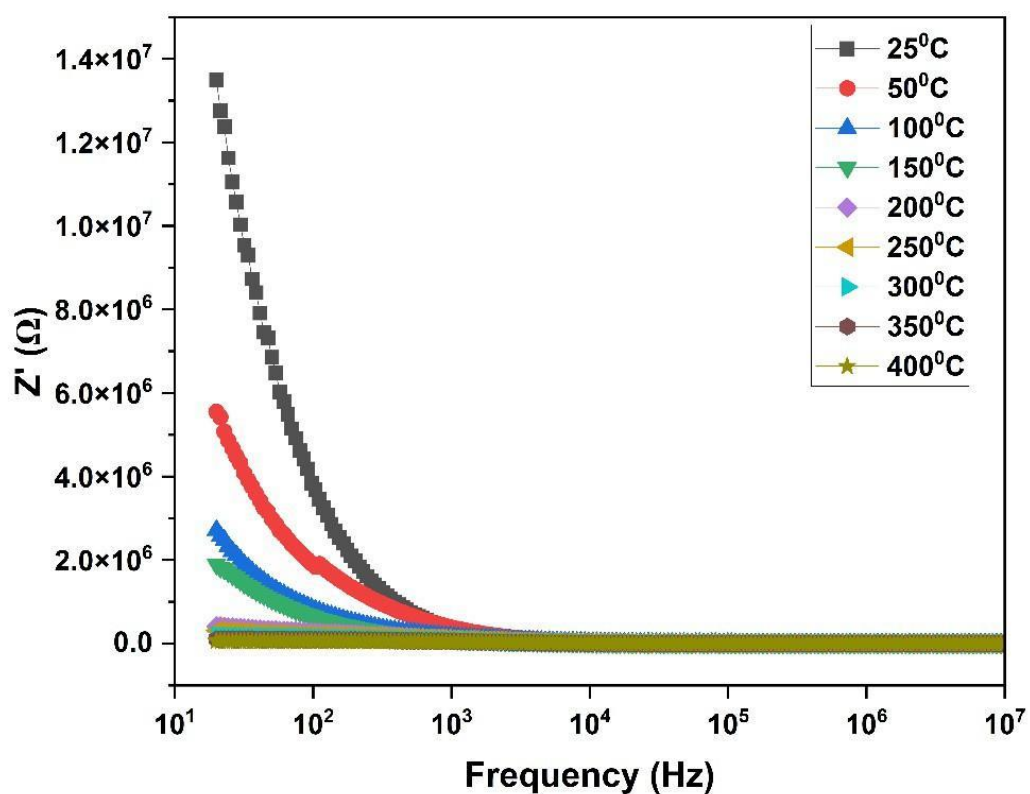


Figure 5: Variation of Real part ( $Z'$ ) of impedance with frequency for  $\text{Ag}_{0.2}\text{Na}_{0.8}\text{NbO}_3$  at various temperatures

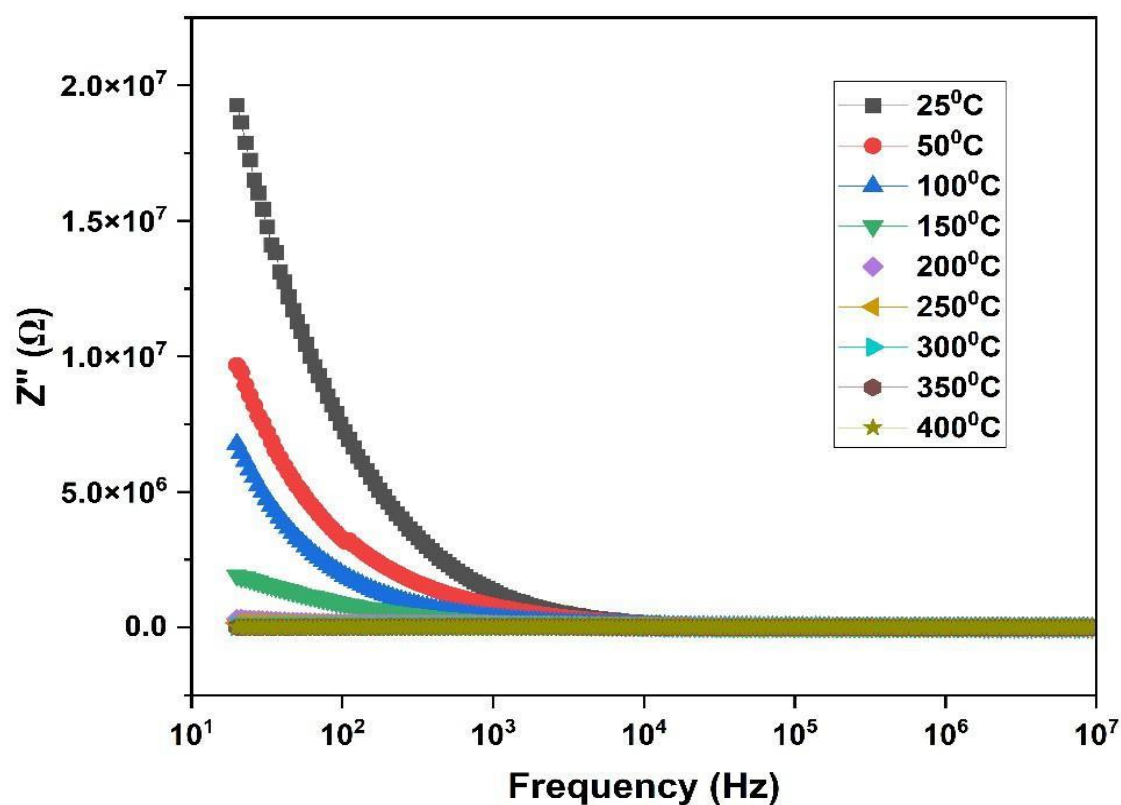


Figure 6: Variation of imaginary part ( $Z''$ ) of impedance with frequency for  $\text{Ag}_{0.2}\text{Na}_{0.8}\text{NbO}_3$  at various temperatures

At a particular frequency, both  $Z'$  and  $Z''$  have been found to drop as temperature rises due to rise in hopping rate of charge carriers.

**Nyquist Plot-** Ceramics have regions like grains, grain boundaries and interfaces possessing different electrical properties.[8] Nyquist plot ( $Z''$  versus  $Z'$ ) of prepared sample has been plotted over wide frequency range corresponding to room temperature as shown in figure 7.

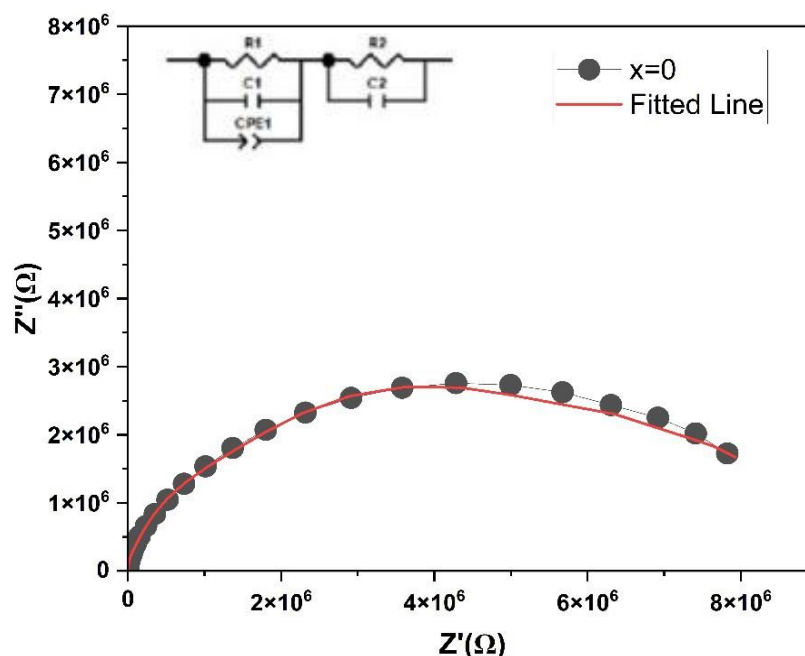


Figure 7: Nyquist Plot of Ag<sub>0.2</sub>Na<sub>0.8</sub>NbO<sub>3</sub>

Obtained plot is in the form of a single semicircle revealing the resistive/capacitive behavior of specimen. For better understanding, obtained data has been fitted with the help of ZSimpWin software using a suitable electrical equivalent circuit. This circuit is shown in inset of figure

7. This is in the form of a combination of two parallel arrays ( $R_1C_1Q$ ) and ( $R_2C_2$ ) connected in series to each other. Here Q represents constant phase element. First and second array show respectively the effect of grains and grain boundaries on conduction process. Fitted line is shown by red semicircle and is found to be in good agreement with the obtained experimental plot. Observed results indicate that obtained semicircle actually arises due to overlapping of two semicircular arcs. First arc observed corresponding to high frequency region represents grain effect and second arc obtained corresponding to low frequency region illustrates the grain boundaries effect. Hence it can be concluded that both grains as well as grain boundaries are contributing towards the electrical properties of sample. The values of all elements present in equivalent circuit  $R_g$  ( $R_1$ ),  $C_g$  ( $C_1$ ),  $R_{gb}$  ( $R_2$ ) and  $C_{gb}$  ( $C_2$ ) and constant phase element (CPE) Q obtained by fitting have been found to be  $1907 \Omega \cdot \text{cm}^2$ ,  $6.211 \text{ E-}6 \text{ F/cm}^2$ ,  $6.591 \text{ E}6 \Omega \cdot \text{cm}^2$ ,  $4.253 \text{ E-}11 \text{ F/cm}^2$  and  $2.540 \text{ E-}7$  respectively.

Observations indicate that the contribution of grain boundaries is more dominant towards the conduction process as value of grain boundary resistance  $R_{gb}$  is much higher as compared to value of grain resistance  $R_g$ .

**3.4 Ferroelectric Analysis-** Polarization-electric field (P-E) hysteresis loop has been recorded for the prepared specimen at room temperature and it is shown in figure 8.

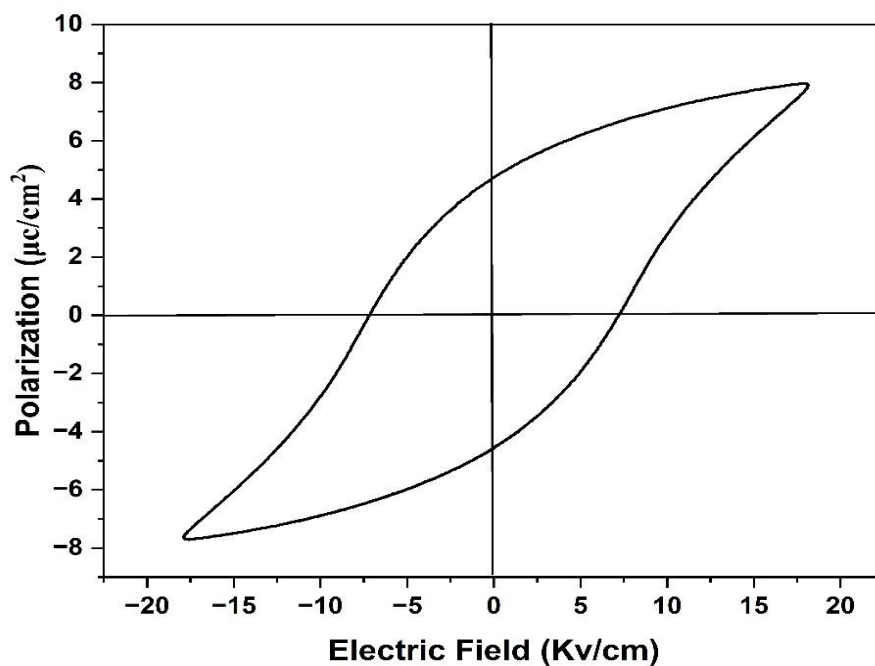


Figure 8: Polarization-Electric Field (P-E) loop of Ag<sub>0.2</sub>Na<sub>0.8</sub>NbO<sub>3</sub>

Although the synthesized ceramic according to its crystal structure is found to be antiferroelectric but still ferroelectric like single hysteresis loop has been recorded. There had been reports in literature previously also which mentioned that a lot of efforts had been put to obtain a proper double hysteresis loop in sodium niobate through many approaches such as by modification of chemical composition [9-11], tailoring of grain size [12,13], variation of temperature [14] and electric treatment of ceramics at high temperature [15]. Peculiar double hysteresis loop featuring antiferroelectricity had been hardly observed in sodium niobate. Pure silver niobate also showed single P-E loop at ambient temperature and low electric field, while it exhibited double hysteresis, when temperature or applied electric field increased. [16] The values of saturation polarization  $P_s$ , remnant polarization  $P_r$  and coercive field  $E_c$  for prepared sample had been observed to be  $7.866 \mu\text{C}/\text{cm}^2$ ,  $4.735 \mu\text{C}/\text{cm}^2$  and  $7.118 \text{ KV}/\text{cm}$ . These values indicate the use of synthesized specimen in non-volatile memory devices.

#### 4. Conclusion

Ceramic pellets of silver sodium niobate Ag<sub>0.2</sub>Na<sub>0.8</sub>NbO<sub>3</sub> prepared through solid-state reaction method have been observed to possess stable perovskite orthorhombic structure by XRD analysis. SEM micrograph confirmed the presence of different sized grains with  $1.65 \mu\text{m}$  average grain size. Grain boundary contribution had been observed to be more dominant as compared to grain contribution to the process of conduction as confirmed by impedance analyzer. Ferroelectric study indicated the presence of single hysteresis loop in the sample. With moderate polarization and high coercive field, specimen is suitable for making non-volatile memory devices,



**References-**

- [1] Ye, J., Wang, G., Chen, X. and Dong, X., 2021. Effect of rare-earth doping on the dielectric property and polarization behavior of antiferroelectric sodium niobate-based ceramics. *Journal of Materiomics*, 7(2), pp.339-346.
- [2] Sharma, D., Chaudhary, S., Rani, M., Jindal, S., Kumar, S. and Dalal, J., 2025. Optimizing structural and magnetic properties of sodium niobate ceramics via Fe and Cu Co-doping for multifunctional applications. *Discover Materials*, 5(1), p.49.
- [3] Alkoy, E.M., Yavuz, A.B., Avdan, D. and Alkoy, S., 2012, July. Electrical properties and impedance spectroscopy of modified potassium sodium niobate ceramics. In *Proceedings of ISAF-ECAPD-PFM 2012* (pp. 1-4). IEEE.
- [4] Soheli, S.N., Lu, Z., Sun, D. and Shyha, I., 2024. Lead-free NaNbO<sub>3</sub>-based ceramics for electrostatic energy storage capacitors. *Ceramics*, 7(2), pp.712-734.
- [5] Yang, L., Kong, X., Li, Q., Lin, Y.H., Zhang, S. and Nan, C.W., 2022. Excellent energy storage properties achieved in sodium niobate-based relaxor ceramics through doping tantalum. *ACS Applied Materials & Interfaces*, 14(28), pp.32218-32226.
- [6] Tania, Chaudhary, S. and Jindal, S., 2024. Structural, optical and magnetic investigations of silver-modified sodium niobate (Na (1-x) Ag<sub>x</sub>NbO<sub>3</sub>)(x= 0.00, 0.01, 0.05) antiferroelectric ceramics for energy storage applications. *Interactions*, 245(1), p.143.
- [7] JCPDS Data Card Number 01-082-0606
- [8] Yang, L., Kong, X., Li, F., Hao, H., Cheng, Z., Liu, H., Li, J.F. and Zhang, S., 2019. Perovskite lead-free dielectrics for energy storage applications. *Progress in Materials Science*, 102, pp.72-108.
- [9] Ye, J., Wang, G., Chen, X., Cao, F. and Dong, X., 2019. Enhanced antiferroelectricity and double hysteresis loop observed in lead-free (1-x) NaNbO<sub>3</sub>-xCaSnO<sub>3</sub> ceramics. *Applied Physics Letters*, 114(12).
- [10] Guo, H., Shimizu, H., Mizuno, Y. and Randall, C.A., 2015. Strategy for stabilization of the antiferroelectric phase (Pbma) over the metastable ferroelectric phase (P21ma) to establish double loop hysteresis in lead-free (1-x) NaNbO<sub>3</sub>-xSrZrO<sub>3</sub> solid solution. *Journal of Applied Physics*, 117(21).
- [11] Qi, H., Xie, A., Fu, J. and Zuo, R., 2021. Emerging antiferroelectric phases with fascinating dielectric, polarization and strain response in NaNbO<sub>3</sub>-(Bi<sub>0.5</sub>Na<sub>0.5</sub>)TiO<sub>3</sub> lead-free binary system. *Acta Materialia*, 208, p.116710.
- [12] Koruza, J., Groszewicz, P., Breitzke, H., Buntkowsky, G., Rojac, T. and Malič, B., 2017. Grain-size-induced ferroelectricity in NaNbO<sub>3</sub>. *Acta Materialia*, 126, pp.77-85.
- [13] Shiratori, Y., Magrez, A., Dornseiffer, J., Haegel, F.H., Pithan, C. and Waser, R., 2005. Polymorphism in micro-, submicro-, and nanocrystalline NaNbO<sub>3</sub>. *The Journal of Physical Chemistry B*, 109(43), pp.20122-20130.
- [14] Shimizu, H., Guo, H., Reyes-Lillo, S.E., Mizuno, Y., Rabe, K.M. and Randall, C.A., 2015. Lead-free antiferroelectric: x CaZrO<sub>3</sub>-(1-x) NaNbO<sub>3</sub> system (0 ≤ x ≤ 0.10). *Dalton Transactions*, 44(23), pp.10763-10772.
- [15] Tan, X., Xu, Z., Liu, X. and Fan, Z., 2018. Double hysteresis loops at room temperature in NaNbO<sub>3</sub>-based lead-free antiferroelectric ceramics. *Materials Research Letters*, 6(3), pp.159-164.
- [16] Gao, J., Zhao, L., Liu, Q., Wang, X., Zhang, S. and Li, J.F., 2018. Antiferroelectric-ferroelectric phase transition in lead-free AgNbO<sub>3</sub> ceramics for energy storage applications. *Journal of the American Ceramic Society*, 101(12), pp.5443-5450.